

Contents lists available at [ScienceDirect](https://www.sciencedirect.com)

Quaternary International

journal homepage: www.elsevier.com/locate/quaint

Heterogeneous vegetation sensitivity at local and regional scales: Implications for pollen-based climate reconstruction

Wei Ding^a, Qinghai Xu^{b,*}, Tian Fu^c, Chunmei Ma^{d,**}, Pavel E. Tarasov^a^a Institute of Geological Sciences, Palaeontology, Free University of Berlin, Berlin, 12249, Germany^b College of Resources and Environment, Hebei Normal University, Shijiazhuang, 050024, China^c Hubei Academy of Forestry, Wuhan, 430075, China^d School of Geographic and Oceanographic Sciences, Nanjing University, Nanjing 210046, China

ARTICLE INFO

Keywords:

Calibration set
East Asian summer monsoon
Human adaptation
Modern analogue technique
MODIS
Vegetation sensitivity index

ABSTRACT

Vegetation–climate relationships are often different at varying spatial scales, which is seldom taken into account in reconstructing past climate changes from fossil pollen spectra represent more local vegetation composition but using regional or extra-regional modern pollen–climate calibration set. In this paper, we employ 2620 surface pollen spectra and six pollen sequences from continental East Asia to reconstruct Holocene climate with modern analogue technique. A novel data set of vegetation sensitivity index (VSI) is introduced to examine vegetation–climate relationships in 0.5° search windows around the fossil sites (local) and in the tailored calibration sets (regional). Then, we compare them to the explanatory abilities of (reconstructed) climate variables on explaining the pollen variance in calibration sets and in the fossil pollen data sets using constrained ordination, cross-validation and significance test. By this procedure that we called local–regional–fossil comparison, we can better determine which variable reconstruction is valid and useful. In our cases, moisture variable reconstructions in temperate forest–steppe ecotone at the East Asian summer monsoon margin are reliable. Consistent Holocene moisture variations with a strong monsoon influence during 8.6–4.0 cal ka BP which can help us to better interpret human adaptations along the Great Wall. However, quantitative climate reconstructions at some sites are less reliable due to highly heterogeneous vegetation sensitivities surrounding the site, particularly for areas with complicated topographical contexts. We stress that vegetation sensitivities at local and regional scales both need to be investigated before conducting quantitative climate reconstruction.

1. Introduction

Pollen analysis is commonly used in palaeoclimate studies with the advantages of availability in most Quaternary sediments and relatively clear ecological implications (Birks and Birks, 1980). Quantitative climate reconstructions using pollen data have already provided us with valuable insights into past climate changes at different parts of our planet at varying spatial-temporal scales (e.g. Chen et al., 2015; Davis et al., 2003; Leipe et al., 2015).

Transfer functions, analogue matching and any other numerical inference models developed for quantitative reconstructions are essentially based on an assumption that modern pollen–vegetation–climate relationships can be extrapolated into the past (Birks et al., 2010). Climate change is recognized as the ultimate driver of ecosystem dynamics and fossil pollen assemblages derived from sediments can well reflect past vegetation composition and structure variations in response

to climate change (Birks and Birks, 1980; Edwards et al., 2017; Jackson and Blois, 2015). This is by no means certain that quantitative climate reconstructions using pollen data will be always plausible. Ecological resilience and thresholds for vegetation communities (not) in response to climate changes are complicated (Jackson, 2006; Willis et al., 2010) and climatic signals are often mixed in pollen spectra and separating them remains difficult (Bennett and Willis, 2001; Huntley, 2012).

Vegetation distribution is restricted by many constraints of which climate variables play different roles in a given region (Prentice et al., 1992). For East Asia, it has more complicated patterns of vegetation–climate relationship for its diverse landscapes from tropical to subtropical, temperate and boreal forests, steppe and desert, as well as vertical vegetation belts due to complex terrain conditions (Hong and Blackmore, 2015; Song and Da, 2016). Pollen-inferred regional differences of past vegetation dynamics in East Asia have been synthesized in many studies (Tian et al., 2016; Wang and Feng, 2013; Zhao and Yu,

* Corresponding author.

** Corresponding author.

E-mail addresses: xuqinghai@mail.hebtu.edu.cn (Q. Xu), chunmeima@nju.edu.cn (C. Ma).<https://doi.org/10.1016/j.quaint.2018.07.002>Received 16 February 2018; Received in revised form 27 June 2018; Accepted 2 July 2018
Available online 02 July 2018

1040-6182/ © 2018 Elsevier Ltd and INQUA. All rights reserved.

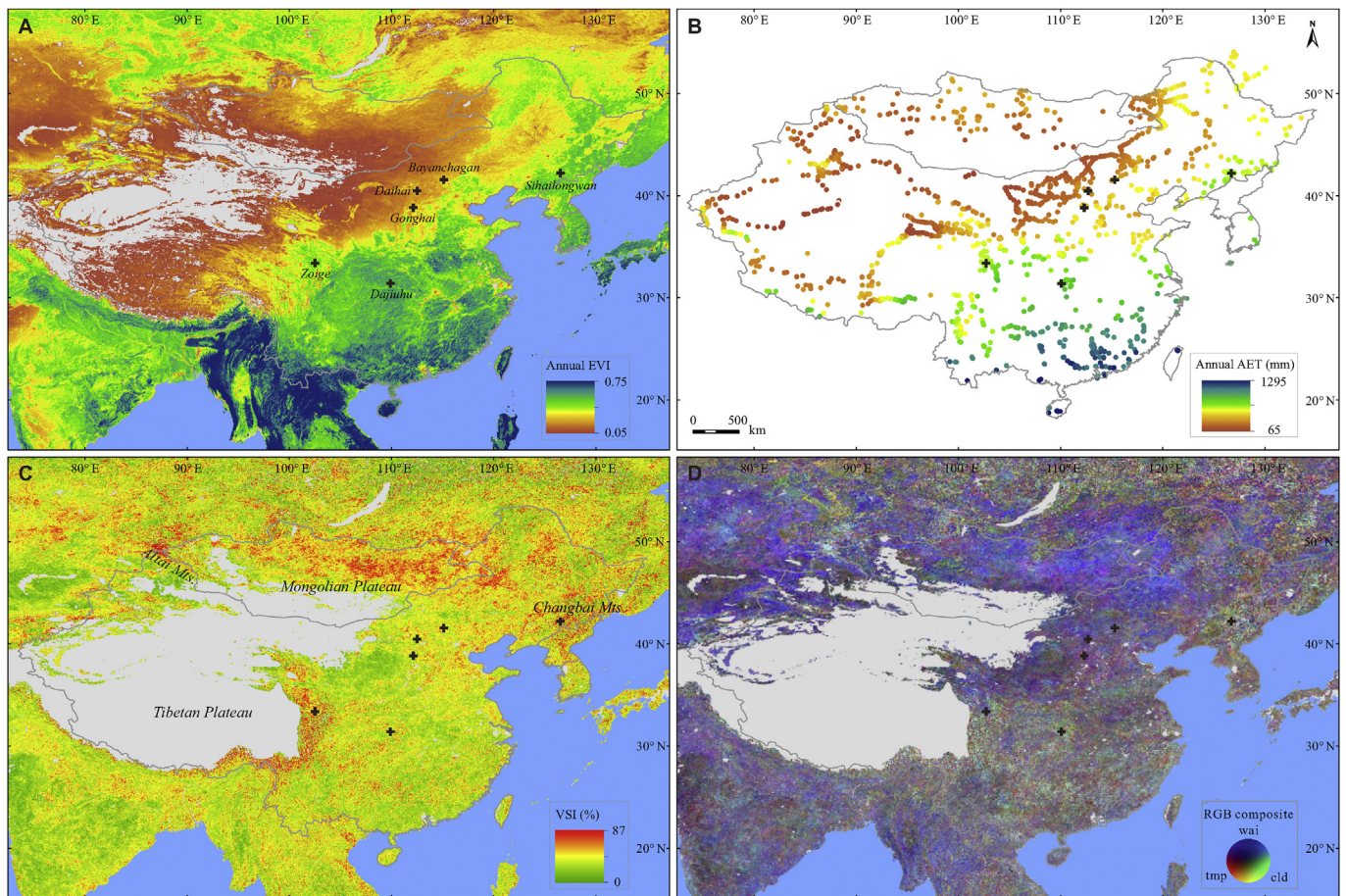


Fig. 1. Pollen sites and vegetation: (A) mean annual enhanced vegetation index (EVI) map with six fossil pollen sites; (B) sketch pattern of mean annual actual evapotranspiration (AET) showing with 0.25° (~ 28 km) buffer zones at 2631 surface pollen sites; (C) vegetation sensitivity index (VSI) pattern; (D) RGB composite of contribution of three climate variables in VSI (tmp: temperature, red; cld: cloudiness, green; wai: water availability, blue). Pixel resolutions are all 0.05° (~ 5.6 km). VSI maps for continental East Asia are extracted from (Seddon et al., 2016). MOD13C2 EVI data are available at the Land Processes Distributed Active Archive Center (<https://lpdaac.usgs.gov>) and MOD16A2 ET data can be accessed from Numerical Terradynamic Simulation Group at University of Montana (<http://www.ntsug.umt.edu>). (For interpretation of the references to color in this figure legend, the reader is referred to the Web version of this article.)

2012) and explanatory abilities of climate variables in regional modern pollen distributions have also been widely discussed (e.g. Li et al., 2015a; Lu et al., 2011). The term of “regional” here means a broad biogeographic area which usually shares a common biome, ecoregion or macroclimate and sometimes even with sociopolitical features (Forman, 1995; Olson et al., 2001; Prentice et al., 1992). However, terms in ecology for different spatial scales (e.g. ecosystem, biotope and niche) all imply a concept of spatial heterogeneity (Forman, 1995). Individual species or plant communities are often distributed in form of scattering patches, for example, *Picea brachytyla* forest patches are often inlaid in the *Abies fargesii* forests above 2300 m of the Shennongjia Mountains in central China which lower parts are dominated by the subtropical broadleaf evergreen and deciduous forests (Hong and Blackmore, 2015; Liu et al., 2015). Encompassing patches within patches, vegetation covers the land like varying-scale uneven mosaics. Recent vegetation surveys and satellite observations have offered us new knowledge on vegetation–climate relationships at different scales, for example, species distributions of dominant, subordinate and rare are often controlled by different factors and vegetation response to climatic variables are quite different even within the landscape due to mosaic-like vegetation sensitivities (Ackerly et al., 2015; Shen et al., 2015).

It means that vegetation–climate relationships within a region may be quite different at finer scales (e.g. local scale) with areas of hundreds of meters to a few tens of kilometers. This has caused less attention in pollen diagram interpretations or quantitative climate reconstructions

in recent palynological studies. Moderate resolution imaging spectro-radiometer (MODIS) on-board the satellites can provide consistently vegetation and climate monitoring at fine mosaic resolution (Huete et al., 2002). Seddon et al. (2016) developed a global data set of vegetation sensitivity index (VSI) using MODIS enhanced vegetation index (EVI) and MODIS-derived air temperature, water availability and cloud cover data. VSI pattern clearly demonstrates that contemporary vegetation response to climate change exists strongly heterogeneous sensitivities at both regional and local scales. Using VSI data set (Seddon et al., 2016) to assess the determinant climate variables for vegetation at a target site and its relevant region may assist us to obtain a more reliable climate reconstruction from pollen data.

Reliably climate reconstructions, in particular for monsoonal China during the Holocene interval, will help us to answer many crucial questions on past human–environment interactions including environmental condition change for inhabitants, human adaptive strategy selection, prehistoric culture evolution and agricultural origins (Ding et al., 2017; Dong et al., 2017; Lu, 2017). In this study, we used 2620 modern pollen spectra from continental East Asia (Zheng et al., 2014) together with 1-km gridded meteorological climate data (Fick and Hijmans, 2017) and MODIS evapotranspiration data (Mu et al., 2011) to establish pollen–climate calibration sets for three moisture variables (annual precipitation, actual evapotranspiration and water availability index) and three temperature variables (annual temperature and temperature of the coldest month and the warmest month). Using modern

analogue technique (Overpeck et al., 1985) and significance test (Telford and Birks, 2011), we reconstructed Holocene climate quantitatively from six well-dated fossil records, including three from sensitive forest-steppe ecotone in North China and three from north-east China, central China and eastern Tibetan Plateau representing different vegetation regions. Meanwhile, VSI data (Seddon et al., 2016) and shuttle radar topography mission (SRTM) elevation data were employed to interpret the quantitative reconstruction results. Our main goals are to (1) evaluate the influences from vegetation sensitivities at the specific site and relevant region on variables selection in pollen-based quantitative climate reconstructions; and (2) interpret culture adaptation along the forest-steppe ecotone in North China during the Holocene with our reliably reconstructed annual precipitation and archaeological data.

2. Study area

Continental East Asia (18°N–54°N, ~3500 km; 73°E–135°E, ~5000 km) encompasses territories of China, Mongolia, and Korean Peninsula (Fig. 1). Geographically, it extends from the western Pacific coast areas (including Hainan, Taiwan and Jeju islands) to the remotely inland Jungar Basin, Tarim Basin and Altai Mountains. The south-eastern part of the study area is controlled by the Asian monsoons which carry moisture from the Pacific and Indian Oceans, while the north-western part is influenced by the Westerlies and moisture from the Atlantic side is mostly intercepted by mountain ranges at the west (Fu et al., 2008; Gunin et al., 1999). This makes the south-eastern part well vegetated but the north-western part mostly covered by the broad deserts (e.g. the Gobi and Taklamakan). The extensive latitudinal gradients, sea-land distance and fluctuant underlying surface within study area define not only the complicated climate settings but also the diverse vegetation types (Gunin et al., 1999; Hong and Blackmore, 2015; Park, 2011).

North China (NC), a vast region from Qin Mountains-Huai River Line (~33°N) to the south-eastern Mongolian Plateau in the north and from coastal areas to the north-eastern margin of Tibetan Plateau (TP) in the west, is particularly important in study area for its sensitive vegetation response to East Asian summer monsoon (EASM) and long-lasting human activities. It has most of the warm temperate forests and temperate steppe in the Continental East Asia (Editorial Committee of Vegetation Map of China, 2007) and it includes Loess Plateau and the most part of the Yellow River Valley which both are tied up with Chinese civilization. Palynological records from NC are often used to portray the EASM rainfall variations (e.g. Chen et al., 2015), particularly at forest-steppe ecotone where present annual precipitation is around 400 mm. Meanwhile, archaeological data from NC including prehistoric cultures evolution in its heartland (i.e. Central China Plains) and agro-pastoral adaptations in its margin (i.e. along the Great Wall) are vital for understanding long-term human-environment interactions from Neolithic to historical times.

3. Data and methods

3.1. Vegetation sensitivity index

Seddon et al. (2016) established a vegetation sensitivity index (VSI) data set to assess the global ecosystems sensitivity to climate change (Fig. 1). This novel and empirical VSI is calculated based on four monthly 0.05° resolution MODIS products, including MOD13C2 EVI data as vegetation productivity, MOD07L2 atmospheric profile product for air temperature, MOD16A2 evapotranspiration product for water availability, and MOD35L2 cloud mask product for cloud-cover as an incoming radiation proxy. EVI has a practical range of 0–1 to indicate increasing green from no vegetation to maximum cover (Fig. 1). VSI for each pixel is calculated based on the monthly mean-variance relationship between EVI and three climate variables and their relative

weights during 2000–2013. Relative coefficients of three climate variables (hereafter as climate coefficients) are rescaled between 0 and 100% using the minimum and maximum values of individual variables and values can be compared directly for a same variable but relatively among the variables. Spatial pattern of three climate coefficients is shown in an RGB composite map (Fig. 1). VSI and climate coefficients are used in this study to examine the determinative climate variables at a specific site and its relevant region (calibration set). Detailed method and data source about VSI are recommended to read in Seddon et al. (2016).

3.2. Modern pollen and climate data

A comprehensive modern pollen data set including 2858 pollen spectra for East Asia has been recently compiled by Zheng et al. (2014). Here, we update the data set with 624 new available pollen spectra, including 32 from Qaidam Basin (Zhang et al., 2012), 30 from central Inner Mongolia (Xu et al., 2014), 91 from north-east China steppe area (Li et al., 2015b), 31 from southern TP (Ma et al., 2017), 33 unpublished spectra from Hexi Corridor, and 407 digitized samples mainly from southwest China plateaus and south Korea mountains (Appendix 1). The pollen percentage calculation was based on sum terrestrial taxa and the data quality control was processed same as in (Zheng et al., 2014). After excluding sites with obvious human impact, in total of 2631 pollen spectra were included in the calibration set (Fig. 1).

Mean annual temperature (TANN), mean annual precipitation (PANN) and mean temperature of the coldest month (TCO) and warmest month (TWA) at pollen sampling sites were derived from WorldClim climate data version 2 (Fick and Hijmans, 2017). WorldClim 2 data set is interpolated at 1-km grid using monthly station climate data (1970–2000) with covariates including elevation, distance to the coast and MODIS-derived maximum and minimum land surface temperature and cloud cover, which improve the interpolation accuracy particularly for temperature variables at the extreme elevations (e.g. TP).

Water availability index (WAI) used in the VSI calculation is the ratio of actual evapotranspiration to potential evapotranspiration (AET/PET or α) which is often used in biome and climate reconstructions (Prentice et al., 1992; Tarasov et al., 1999). AET is the sum of water lost from the land surface to the atmosphere, includes evaporation from moist soil, canopy interception and water bodies and the transpiration from plant canopy, while PET is a theoretical value estimated as the amount of AET that would occur if a sufficient water source is available. Input data for MODIS ET algorithm include not only meteorological data but also vegetation related data like land cover, biome types and albedo (Mu et al., 2011). In this study, we also used mean annual AET and WAI as moisture variables to establish pollen–climate calibration sets.

EVI values were extracted from a 0.05 arc-degree (0.05°, ~5.6 km) MOD13C2 product (Didan, 2015). ET values were extracted from a 15-year (2000–2014) 0.05° MOD16A2 ET product (Mu et al., 2011). Unvegetated pixels with mean annual EVI < 0.05 in the EVI map and mean EVI < 0.1 for all months in VSI calculation are masked (Fig. 1). We established 0.25° buffer zones for a few samples from desert areas and calculated the mean AET and PET values ignoring NoData pixels using *Zonal Statistics* function in ArcMap (Fig. 1). There are 11 sites which still have no data can be extracted were removed.

3.3. Fossil pollen data

Six well-dated fossil pollen records from monsoonal China with sufficient analogues within 1000 km were selected to conduct Holocene climate reconstructions (Table 1). Lakes Bayanchagan (Jiang et al., 2006), Daihai (Xiao et al., 2004) and Gonghai (Xu et al., 2017) are located on the eastern contiguous area of Inner Mongolian Plateau–Loess Plateau in NC and also in the EASM margin area. Lake

Table 1

Summary information for the six fossil pollen records. Sites latitude (°N), longitude (°E), elevation (m, a.s.l), numbers of radiocarbon dates and pollen samples and compositional turnover (SD, standard deviation units) during the Holocene interval, modern vegetation zone and sub-zone code (Editorial Committee of Vegetation Map of China, 2007) and reference are listed.

Sites	Latitude	Longitude	Elevation	Datings	Samples	Turnover	Modern vegetation	Reference
Bayanchagan	41.635	115.208	1370	9	82	1.34	Southern temperate forest (meadow)-steppe (VIAiia2)	Jiang et al. (2006)
Daihai	40.579	112.703	1219	8	271	1.37	Southern temperate forest (meadow)-steppe (VIAiia3)	Xiao et al. (2004)
Gonghai	38.909	112.234	1860	20	656	1.45	Northern warm temperate deciduous Quercus forest (IIIi8)	Xu et al. (2017)
Sihailongwan	42.287	126.602	777	29	191	1.27	Southern temperate mixed needleleaf and deciduous broadleaf forest (IIIi1)	Stebich et al. (2015)
Dajiuhu	31.491	109.996	1752	6	105	1.55	Northern subtropical broadleaf evergreen and deciduous forest (IVAi4)	Zhu et al. (2010)
Zoige	33.450	102.633	3467	8	153	0.97	Subalpine scrub and alpine meadow (VIIIi1)	Zhao et al. (2011)

Sihailongwan (Stebich et al., 2015) lies to the west of Changbai Mountains in north-east China. Dajiuhu peatland (Zhu et al., 2010) is located in Shennongjia Mountains and the middle reaches of the Yangtze River. Zoige peatland (Zhao et al., 2011) is situated on the eastern TP. The sequence from Zoige Peatland represents the last 10.3 cal ka BP (thousands of years before AD 1950) and the others cover the entire Holocene interval (~11.7 cal ka BP). Except Lake Daihai which had an area of 160 km², the pollen sequences from other three small lakes (0.18–15 km²) and two peatlands recorded more local vegetation composition. Six sites from four different vegetation regions are used for inter-regional comparisons and three sites within NC are used for intra-regional comparisons. Sites location, vegetation types and more information are listed in Table 1.

To obtain specific site information, we extracted monthly EVI, VSI coefficients and SRTM elevation data around six fossil sites using a 0.5° × 0.5° (~56 km at the equator) search window. For sites which surrounding area now mostly covered by cultivated vegetation, we shifted the search windows for EVI and VSI to adjacent areas (within 50 km) to catch more natural vegetation characteristics. VSI coefficients at search windows were used to evaluate the vegetation–climate relationships at local scales, while VSI coefficients at pixels of surface pollen sites in calibration sets are used for regional evaluation. SRTM 1 arc-second (~30 m) data are available at the US Geological Survey website (<https://ita.cr.usgs.gov/srtm1arc>).

3.4. Numerical methods

We used modern analogue technique (MAT) to establish the calibration sets between pollen and climate variables (TANN, TCO, TWA, PANN, AET and WAI). MAT has advantages of ecological plausible and no assumed response model (Birks et al., 2010) and it has been successfully applied in many pollen-based quantitative climate reconstructions (e.g. Davis et al., 2003; Leipe et al., 2015). Due to taxonomic resolution is mostly identified at genus or family levels, similar pollen assemblages (analogues) may originate from vegetation communities under different climatic conditions (Birks et al., 2010). Cao et al. (2017) suggested that calibration sets for Holocene climate reconstructions in China should be restricted to the spatial extent with a radius of 1000–1200 km. In this study, we customized calibration sets for each fossil site with a geographical distance constraint. Surface samples beyond the radii of 1200 km from the fossil site are not used in the customized data sets. To optimize the signal-to-noise ratio, taxa which present in at least 2% of the total samples in tailored data sets were selected for MAT models. MAT estimates of past climate were derived from weighted averages of modern climate variables at the five closest analogues (Overpeck et al., 1985).

To obtain valid and useful reconstructions, we made two-step tests for all variables. First, using redundancy analysis (RDA) or canonical correspondence analysis (CCA; when compositional turnover more than 3) to assess the proportion of pollen variances explained by the climate variables in the modern training-sets and leave-one-out cross-validation to assess the model accuracy. Then, using RDA (low compositional

turnover in fossil data) to assess the pollen variances explained by reconstructed climate variables and using the randomisation technique (999 random environmental variables) to assess the statistical significance (Birks et al., 2010; Salonen et al., 2014; Telford and Birks, 2011). The length of the first axis (SD: standard deviation units) in detrended correspondence analysis (DCA) for the pollen data set is estimated as compositional turnover (Hill and Gauch, 1980; Telford and Birks, 2011). The ratio of first constrained to first unconstrained axis (λ_1/λ_2) in RDA or CCA is used to state the relative explanatory power of a climate variable (Juggins, 2013). Reconstructions for variables that have λ_1/λ_2 values less than 1 should be carefully interpreted. The first step normally is used to select appropriate variables, in this study, we conducted reconstructions for all six variables without immediate selections. Then, we compared the results of VSI climate coefficients around the fossil sites (vegetation–climate relationships at local scale) and in the calibration sets (regional scale), pollen–climate relationships in calibration sets and significance test results of climate reconstructions (pollen–climate relationships in the fossil data). Simplify, we named this as local–regional–fossil comparison.

All data analyses were performed in R environment (R Core Team, 2016). Geographic distance between modern and fossil sites were calculated using the *rdist.earth* function in the *fields* package version 9.0 (Nychka et al., 2016). Significance tests were carried out using *randomTF* function in the *palaeoSig* package version 1.1–3 (Telford, 2015). Ordinations and MAT were made using *vegan* package version 2.3–5 (Oksanen et al., 2016) and *rioja* package version 0.9–15 (Juggins, 2015).

4. Results

4.1. Heterogeneous vegetation sensitivity at local and regional scales

The medians and interquartile ranges of monthly EVI and VSI coefficients in boxplots indicate that the vegetation growth and sensitivity to climate are complicated in a given search window (Fig. 2). Monthly EVI at six fossil sites show a similar temporal pattern of the growing season but with regional and site-specific characteristics (Fig. 2A). EVI values increase obviously in May at Lakes Bayanchagan, Daihai and Gonghai from the temperate forest-steppe ecotone but reach their maximum slightly different in July–August, while Lake Sihailongwan in temperate mixed forest has larger variations in May. This process for Dajiuhu Peatland from evergreen-deciduous broad-leaved forest ecotone is about one month earlier in April and all monthly values are 0.1–0.2 higher. The maximum monthly EVI at Zoige Peatland on eastern TP is observed in July but the beginning of growing season is one month lagged comparing to Dajiuhu Peatland which has close latitude.

Climate coefficients of mosaic vegetation around the fossil sites (search windows) and surface pollen sites in calibration sets demonstrate intra- and inter-regional similarities and differences (Fig. 2B). Lakes Bayanchagan, Daihai and Gonghai have higher coefficient medians for water availability and less for cloudiness comparing to

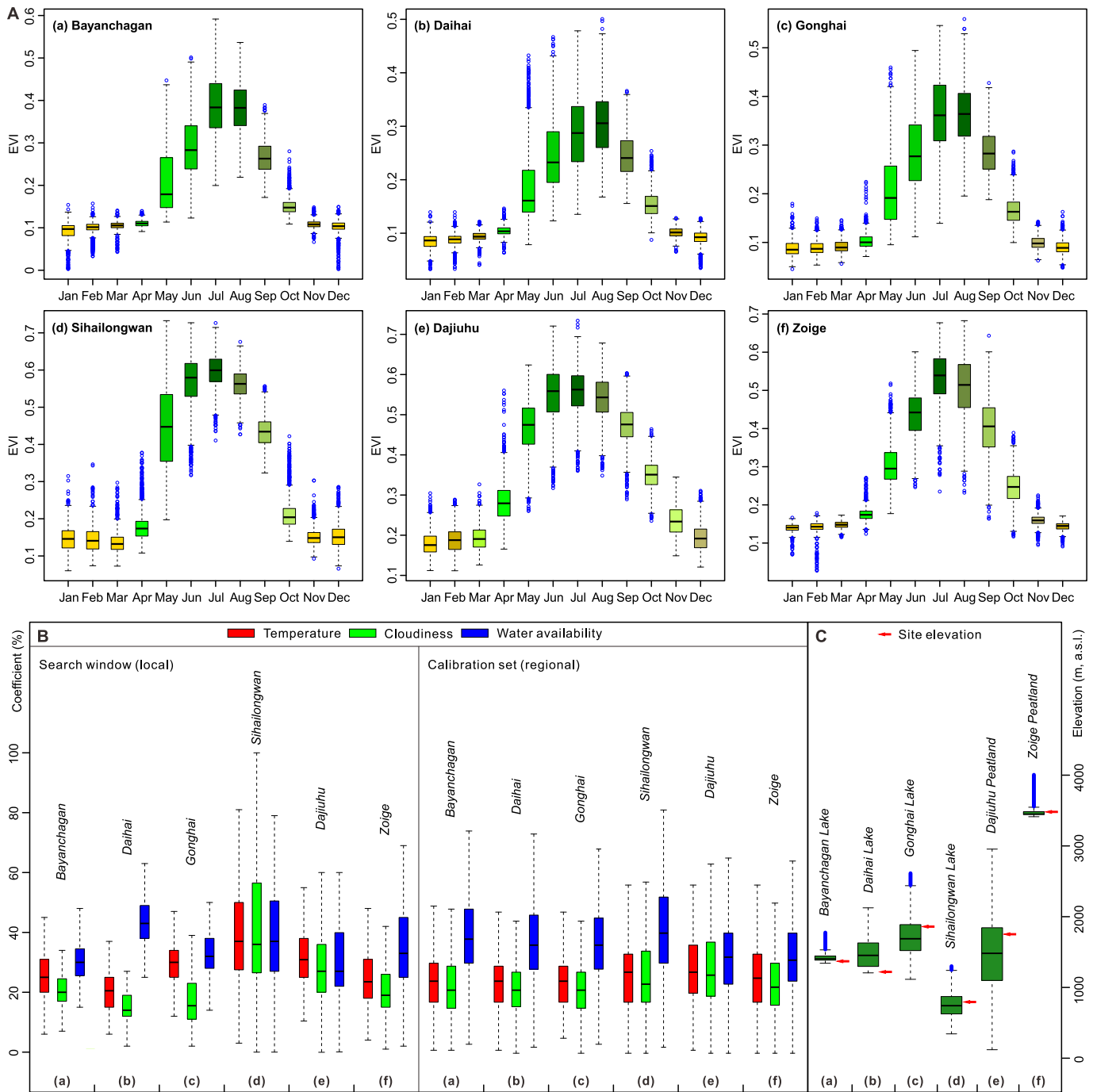


Fig. 2. (A) Mean monthly enhanced vegetation index (EVI) patterns showing with a yellow–green color range; (B) Relative coefficients of temperature, cloudiness and water availability in vegetation sensitivity index (VSI) in search windows and calibration sets; (C) SRTM elevation ranges around the sampling sites. Statistics for 0.5° search windows are based on 100 pixels (~5.6 km) for EVI (by 14 years) and VSI data and 3240000 pixels (~30 m) for SRTM data. All boxplots show the median, interquartile range, minimum, maximum and some with outliers. (For interpretation of the references to color in this figure legend, the reader is referred to the Web version of this article.)

temperature. The interquartile ranges for three sites are shorter which means vegetation sensitivities to a same climate variable are relative close in surrounding patches. Lake Sihailongwan has large interquartile ranges of three climate coefficients which indicates highly heterogeneous vegetation sensitivities. Vegetation at Dajiuhu Peatland is sensitive more to cloudiness and temperature and temperature coefficient is slightly higher. Zoige Peatland has similar pattern (higher WAI coefficient) with NC sites.

WAI coefficients in tailored calibration sets generally have higher medians and larger interquartile ranges compare to temperature and

cloudiness coefficients which indicate vegetation mosaics are more sensitive to moisture variations at regional scale. However, WAI coefficients in calibration sets for Peatlands Dajiuhu and Zoige are relative lower than four northern sets. Coefficient patterns of Lake Sihailongwan and Dajiuhu Peatland in search windows are not well consistent with their calibration sets. The SRTM elevation patterns around the sampling sites are shown in (Fig. 2C). Dajiuhu area has the most complicated topography in our cases.

Table 2

Summary statistics for MAT model (5 closest analogues) performance of six climate variables in six tailored data sets. Numbers of surface pollen sites (size), pollen taxa used and compositional turnover in calibration sets are given. Pollen variance (%) explained by variables as a sole predictor and the ratio of first constrained to first unconstrained axis (λ_1/λ_2) in RDA or CCA are listed. Values of λ_1/λ_2 greater than 1 are shown in bold and greater than 0.8 are marked with asterisks. Root mean square error of prediction (RMSEP) and coefficient of determination (r^2) between observed and predicted values produced by the leave-one-out cross-validation are listed.

Data sets	Bayanchagan	Daihai	Gonghai	Sihailongwan	Dajiuhu	Zoige
Size	979	980	997	527	814	538
Taxa	83	86	86	72	107	82
Turnover	2.7	2.8	2.7	2.9	3.6	2.9
RDA and CCA: pollen variance (%) and λ_1/λ_2						
TANN (°C)	3.6/0.12	3.6/0.13	4.3/0.16	10.3/0.41	5.0/0.96*	6.4/0.25
TCO (°C)	3.9/0.13	5.3/0.21	6.5/0.29	11.0/0.46	5.8/1.17	10.5/0.56
TWA (°C)	4.9/0.16	4.9/0.17	6.6/0.25	6.0/0.21	3.6/0.38	8.1/0.32
PANN (mm)	19.6/1.24	17.4/1.15	18.0/1.19	16.5/0.85*	6.8/1.38	17.2/1.13
AET (mm)	20.7/1.27	18.0/1.17	17.9/1.19	16.7/0.80*	6.0/1.21	16.4/0.98*
WAI	20.1/1.16	17.3/1.07	16.5/1.04	15.0/0.62	5.4/1.08	13.1/0.72
Cross-validation: RMSEP and r^2						
TANN (°C)	1.77/0.81	1.92/0.76	1.86/0.77	1.91/0.83	2.19/0.84	1.82/0.77
TCO (°C)	3.05/0.80	3.05/0.77	2.77/0.72	3.06/0.84	2.21/0.87	2.06/0.82
TWA (°C)	1.62/0.76	1.89/0.75	2.09/0.77	1.46/0.73	2.51/0.79	1.46/0.73
PANN (mm)	71/0.89	74/0.86	80/0.85	72/0.93	124/0.91	64/0.90
AET (mm)	52/0.88	59/0.84	59/0.86	49/0.88	66/0.84	55/0.88
WAI	0.045/0.89	0.048/0.81	0.050/0.83	0.048/0.87	0.050/0.84	0.048/0.86

4.2. Assessment of the calibration sets

Summary statistics for 36 calibration models are presented in Table 2. Calibration sets tailored for target fossil sites contain sufficient (500–1000) surface pollen spectra. The compositional turnovers in tailored calibration sets are about 2–3 times of their fossil data sets. Variables performances seemingly have a moisture–temperature different pattern.

Moisture variables generally explain more pollen variances in calibration sets. For NC sites, values of λ_1/λ_2 for moisture variables in RDA are all greater than 1 and temperature variables (TANN, TCO and TWA) are all less than 0.3. Pollen variances explained by moisture variables as a sole predictor are 17–21% while for temperature variables are much less (~4–7%) for NC sites. Comparing to NC sites, moisture variables in Lake Sihailongwan perform slightly worse while temperature variables TANN and TCO perform better. However, the λ_1/λ_2 values for all variables are less than 1. Values of λ_1/λ_2 of moisture variables for Dajiuhu Peatland in CCA are greater than 1 and temperature variables TCO and TANN also perform well. Moisture variables at Zoige Peatland explain more variances than temperature variables.

MAT models inferred climate variables agree well with the observation data using both comprehensive sets for Continental East Asia (Fig. 3) and tailored sets for six fossil sites (Table 2). Root mean square error of prediction (RMSEP) and coefficient of determination (r^2) between observed and predicted values produced by the leave-one-out cross-validation using tailored sets are slightly different comparing to comprehensive sets. Moisture variables have higher r^2 values (~0.81–0.93) than temperature variables (~0.72–0.87) in most calibration sets.

4.3. Holocene climate reconstructions and significance tests

Significance tests results for Holocene climate reconstructions at six sites are presented in Table 3. Maximal variance proportions in fossil pollen assemblages can be explained by a possible reconstruction (i.e. the first axis of a principal components analysis) are 67–80% for NC sites and reconstructed moisture variables usually can explain 40–60% of total variances and all pass the significance tests. Temperature variables reconstructions capture less variances in fossil data sets than moisture variables, but TWA in Lake Bayanchagan and TCO in Lakes Daihai and Gonghai pass the significance tests. Reconstructed temperature variables at Dajiuhu explain more fossil pollen variance and

pass the significance tests.

Reconstructed PANN explains very little variance in fossil data of Zoige Peatland on TP and temperature variables explain more variances but relative low comparing to the maximal explainable variance (84.9%). Variables at Lake Sihailongwan have close explanatory power except to WAI. The maximal and explainable variance proportions for Dajiuhu Peatland and Lake Sihailongwan are relative low (39.8% and 48.1%). There are no reconstructions for Zoige Peatland pass the significance tests. Plausible reconstructions are in the supplementary material (Appendix 2) and selected reliable moisture reconstructions at forest-steppe ecotone (pass the local–regional–fossil comparisons) are presented in Fig. 4.

5. Discussion

5.1. Variable selection in pollen-based climate reconstruction

VSI map shows that vegetation on eastern TP, northern Mongolian Plateau, Altai and Changbai Mountains areas are highly sensitive to climate change (Fig. 1C). Generally, grasslands in the north are more moisture limited and forests in the south and north-east China respond more to cloudiness and temperature. RGB composite map clearly exhibits heterogeneous sensitivity of vegetation to climatic variables from mosaic level to local and regional scales (Fig. 1D).

Extracted VSI coefficients pattern in the search windows of fossil sites are not always consistent with those of surface pollen sites in the calibration sets (Fig. 2B). Relative importance of (reconstructed) climate variables on explaining pollen variances in fossil data and in modern calibration sets are also not always consistent (Tables 2 and 3). The inconsistencies between MAT model performances and significance tests (Table 3) seems to be more impacted by local VSI pattern under contemporary conditions and possible climate change in the past. Using the local–regional–fossil comparison, variable reconstructions in our cases can be divided into following three types.

- (1) Reconstruction of a variable is reliable as its greater importance (explanatory power) is always consistent in the local–regional–fossil comparison. WAI coefficients in the search windows and calibration sets both are the highest for NC sites and moisture variables have major explanatory power ($\lambda_1/\lambda_2 > 1$) on pollen variance in tailored calibration sets and reconstructed moisture variables explain significant variance in the fossil data (Juggins,

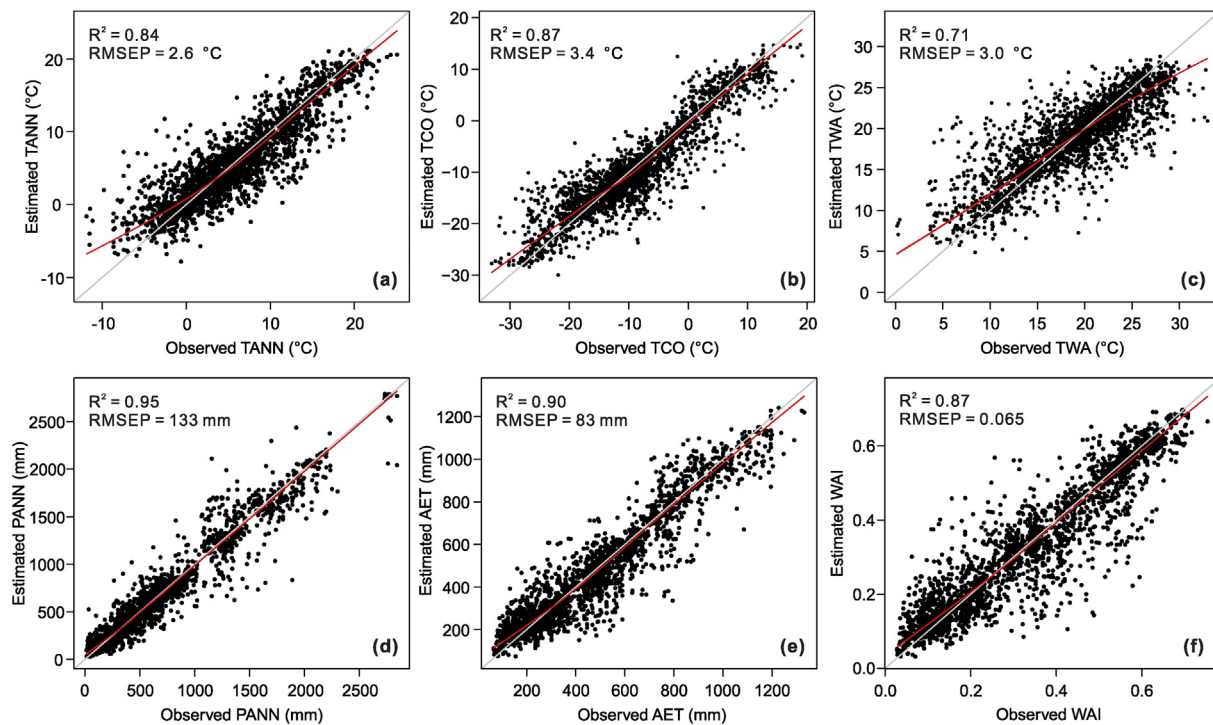


Fig. 3. Comparison of the observation values of six climate variables (TANN, TCO, TWA, PANN, AET and WAI) to the analogue-based estimates at 2620 modern pollen sites from continental East Asia. R^2 is the coefficient of determination between observed and estimated values and RMSEP is the root mean square error of prediction produced by the leave-one-out cross-validation.

Table 3

Summary statistics of Holocene climate reconstructions in significance tests. Pollen variance (%) in fossil data sets explained by reconstructed climate variables are listed. EX.max represents the maximum proportion of the variance (%) in a fossil data set could be possibly explained. Reconstructions passing the significance tests ($p < 0.05$) are shown in bold and variables in calibration sets have λ_1/λ_2 values greater than 1 are marked with asterisks and greater than 0.8 are marked with daggers.

Data sets	Bayanchagan	Daihai	Gonghai	Sihailongwan	Dajiuhu	Zoige
TANN (°C)	1.0	12.6	15.5	26.7	25.5†	19.8
TCO (°C)	9.6	27.8	31.5	28.1	19.2†	19.6
TWA (°C)	42.6	8.2	17.1	17.2	27.2	42.6
PANN (mm)	42.0*	61.1*	58.9*	28.8†	13.5	1.0
AET (mm)	38.0*	48.3*	54.4*	24.3	12.7	3.9
WAI	43.1*	44.4*	52.5*	1.6	15.2	4.0
EX.max	66.6	80.1	76.3	48.1	39.8	84.9

2013; Telford and Birks, 2011). For this situation, it is clear that Holocene moisture reconstructions at these sites can be trusted.

(2) Reconstruction of a variable is relative plausible as its greater importance in local VSI and in the fossil pollen data is consistent and its explanatory power in regional pollen data is acceptable. All variables except TWA for Dajiuhu Peatland have relative high λ_1/λ_2 values (~0.96–1.38) in CCA and moisture variables perform slightly better in calibration set. This is also consistent with the slightly higher WAI coefficient in calibration set. However, temperature coefficient is slightly higher than WAI in search window and temperature variables reconstructions accordingly pass the significance tests while moisture variables explain relative low variances. This is somewhat surprising that result of significance test in fossil data is more related to VSI coefficients pattern in search window (Fig. 2B and Table 3). For this situation, we consider that reconstructions of TANN and TCO for Dajiuhu are relative plausible but moisture reconstructions should be treated with caution. Similarly, temperature variables (TANN and TCO) and

moisture variables (PANN and AET) reconstructions explain similar variance (24–29%) in fossil data from Lake Sihailongwan. This is more related to VSI coefficients in search window rather than pollen (vegetation)–climate relationships extracted from regional calibration set that moisture variables are more important. The λ_1/λ_2 value of 0.85 for PANN in RDA is acceptable due to the relative large size of our calibration set (Salonen et al., 2014) and its reconstruction pass the significance test. Therefore, Holocene PANN reconstruction at Lake Sihailongwan is also useful.

(3) Importance for a reconstructed variable in fossil data is not consistent with its performance in local VSI and regional pollen–climate calibration set. For site Zoige on eastern TP, WAI coefficient is higher in both local and regional VSI and moisture variables in calibration sets also explain more variances, however, reconstructed temperature variables explain more variances in fossil pollen data (Table 3). For example, AET accounts 16.4% pollen variance and λ_1/λ_2 is 0.98 in calibration set but AET reconstruction only explain 3.9% variance in fossil data. A possible reason for this inversion is that thermal condition during the Holocene is more important than present on TP. Zhao et al. (2011) noted that summer insolation induced temperature may has played a major role on Holocene vegetation change in Zoige Basin based on pollen and other multiple proxy data. Vertical vegetation belts shift in montane areas on TP are considered sensitive to temperature changes (Herzschuh et al., 2006; Li et al., 2011). The land in the search window around the sampling site in Zoige Basin is relative flat (~3500 m a.s.l), however, the whole basin is located on the transitional zone from cool-temperate forest to subalpine needle-leaf forest with a steep elevation range and the limiting factor is growing season warmth (Fang et al., 1996). This may interpret that why reconstructed Holocene TWA explains the highest variance (42.6%) in the fossil data. Similarly, TWA explains lowest variance in calibration set for Dajiuhu Peatland but highest in fossil data. For northern sites, reconstructed TWA for Lake Bayanchagan, TCO for Lakes Daihai and Gonghai, and TANN and TCO for Lake

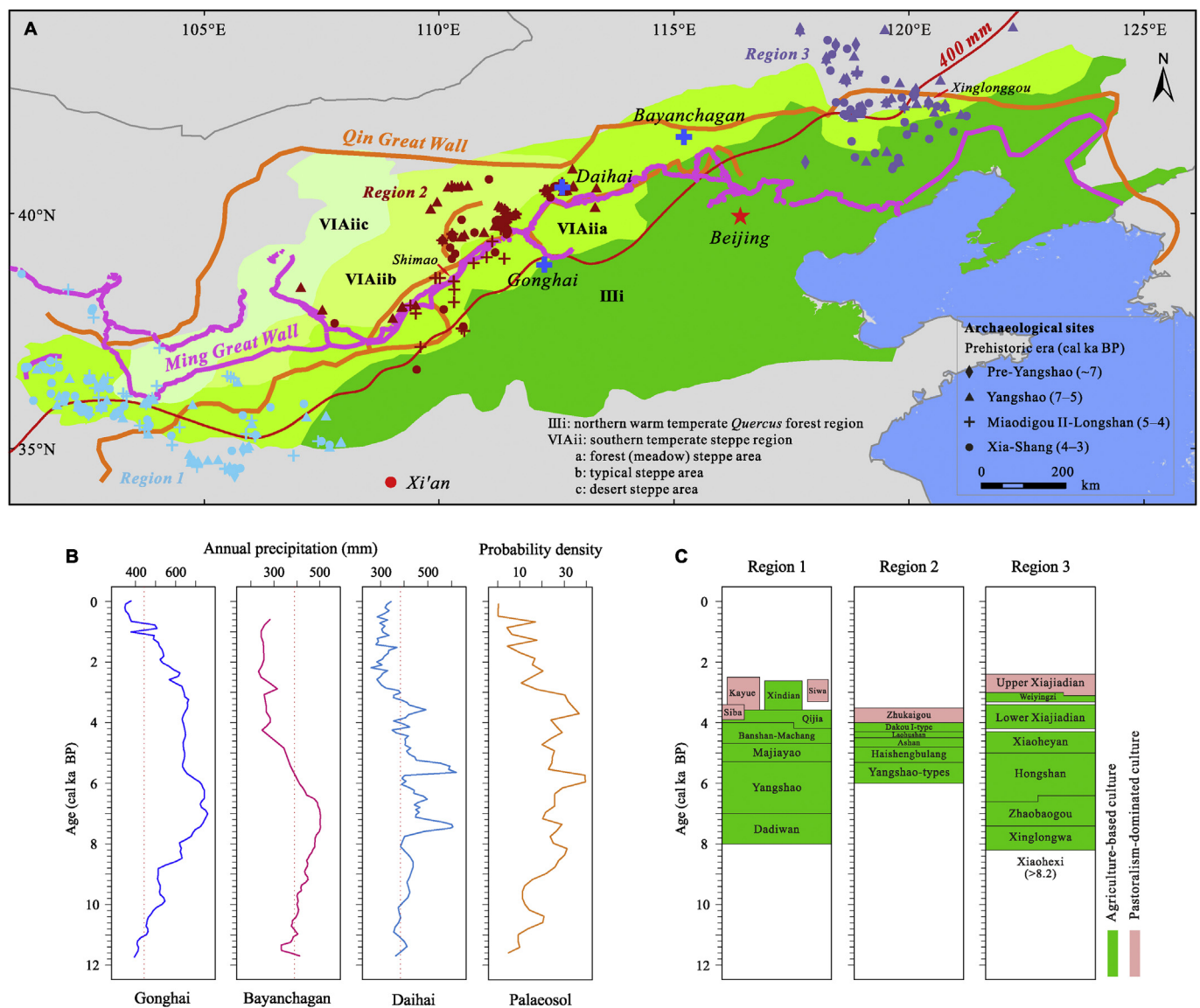


Fig. 4. (A) Distributions of major archaeological sites in forest-steppe ecotone in different stages according to prehistoric cultures evolution in Central China Plains; (B) Holocene annual precipitation reconstructions with LOWESS smoother (span:0.01) for Lakes Gonghai, Bayanchagan and Daihai (dotted lines indicate modern values) and the probability density of palaeosol formation in the Chinese Loess Plateau (Wang et al., 2014); (C) Archaeological culture sequences at three selected regions (IA CASS, 2003, 2004, 2010). Main routes of the Great Wall built in Qin Dynasty (221–206 BCE) and Min Dynasty (1368–1644) are drawn according to real locations of their ruins and 400 mm annual precipitation isohyet is based on meteorological data during 1981–2010, and these lines are often used as geographic boundaries between regions of forest and steppe or agriculture and animal husbandry. Region 1: Gansu-Qinghai (Upper Reaches of Yellow River) culture region; Region 2: Southeastern Inner Mongolian and northern Shanxi and Shaanxi culture region; Region 3: West Liao River Basin culture region. (For interpretation of the references to color in this figure legend, the reader is referred to the Web version of this article.)

Sihailongwan explain significant variances in fossil data but with very low explanatory power in calibration sets. It is hard to determine whether this type of reconstructions can be trusted, nevertheless, the significance tests provided us with new possibility to better interpreting the past climate change using pollen data at a specific site. Before more detailed pollen-vegetation-climate investigations at local scale, we should avoid to conduct quantitative reconstructions of these variables.

In summary, quantitative climate reconstructions using pollen data need to examine not only the regional pollen-climate relationships in the calibration sets but also the local vegetation sensitivity. Both VSI coefficient patterns and pollen-climate relationships for our NC sites indicate that moisture is a limiting factor that affects vegetation growth and distribution in the northern part of monsoonal China (Hong and

Blackmore, 2015; Seddon et al., 2016). VSI patterns in search windows and calibrations sets are consistent for NC sites and moisture variables can explain more variance in both calibration sets and fossil data sets. Therefore, pollen-based Holocene moisture reconstruction for NC can be trusted and used to indicate EASM rainfall variations (Chen et al., 2015). Mosaic vegetation sensitivities to climate variables around the Lake Sihailongwan from temperate mixed needleleaf and deciduous broadleaf forest region are complicated (Fig. 2). Temperature and moisture variables have close VSI coefficients in search window and also explain close variances in fossil data. Comparing to NC sites, moisture is less determinant. The maximum proportion of the explained variance (48.1%) in fossil data is also much lower than three NC sites (66.6–80.1%). Better performances of temperature reconstructions on explaining the fossil pollen variances for Peatlands Dajiuhu and Zoige seems to be related to the vegetation sensitivities caused by local and

regional elevation patterns. It is easy to imagine that vertical vegetation belts shift sensitively in response to the Holocene temperature variations (Fang et al., 1996; Zhao et al., 2011). When vegetation mosaics are sensitive to multiple variables around a specific site, quantitative climate reconstruction from pollen data becomes less plausible. We stress that local VSI pattern is important for climate variable selection in climate reconstruction.

There are many factors that may have influences on numerical analyses results. Separating the roles of climatic variables on Holocene vegetation dynamics is difficult. For example, relative coefficient of cloudiness in VSI indicates that insolation has an important role in vegetation variations particularly for sub-humid and humid forest areas (Fig. 1D), however, quantitative cloudiness (insolation) reconstruction using pollen data is not reliable and somehow ridiculous. It should be aware that backward chaining a certain climate variable quantitatively from pollen (vegetation) data is not always ecologically supported (Juggins, 2013). Nevertheless, vegetation sensitivity is heterogeneous at local and regional scales due to mosaic vegetation distributions and our procedure of the local–regional–fossil comparison can assist one to determine which climate reconstruction is valid and useful.

5.2. Holocene moisture variations at East Asian summer monsoon margin and human adaptation

VSI pattern in study area has clearly demonstrated the heterogeneous vegetation sensitivities to climate change at varying scales (Fig. 1). Ancient culture evolution is also influenced by different environmental factors at varying scales, such as sudden floods at local scale and long-term droughts at regional scale (deMenocal, 2001; Dong et al., 2017). Reliable climate reconstruction for a region or a specific site that pass our local–regional–fossil comparison will help us to better interpret past human behaviour, in particular, the adaptive strategies adopted by prehistoric human in response to environmental condition changes (Jia et al., 2016; Yi et al., 2014). Here, we focus on the forest-steppe ecotone in NC where vegetation mosaics are very sensitive to moisture changes. The ecotone along the present-day EASM margin involves many topics on human–environment interactions, including the Great wall, isohyet 400 mm (Fig. 4A) and farming–pastoral boundary shifts (e.g. Sang et al., 2017). Our Holocene moisture reconstructions (Fig. 4B) can be used to trace past human adaptive responses to EASM precipitation changes (Li et al., 2016; Wagner et al., 2013).

Remarkable rainfall increasing during 8.6–7.8 cal ka BP could have promoted the development of millet agriculture in northern China (Hu et al., 2008; Liu et al., 2012; Wu et al., 2014; Zhao, 2011). The Xinglonggou site in region 3 was an important millet domestication center during 8–7.5 cal ka BP (Liu et al., 2012; Zhao, 2011). Our reconstructions indicate that annual precipitation along the Great Wall and today's isohyet 400 mm for this period were 100–200 mm higher (Fig. 4B). Stable and relatively high precipitation during 7–5 cal ka BP could have provided the environmental basis for the prosperity and expansion of the Yangshao Culture which people subsisted primarily on millet but with a small quantity of rice in the middle reaches of the Yellow River (Institute of Archaeology CASS, 2010). Its influence was widespread to the adjacent areas including southeastern Inner Mongolia Plateau (region 2). Wang et al. (2014) synthesized the probability density of palaeosol formation across the Loess Plateau based on 310 dates from 77 loess–palaeosol sequence and concluded that a strong EASM existed during 8.8–3.4 cal ka BP. This is consistent with our reconstructions. Stable and favorable climatic conditions during the middle Holocene in NC have increased population growth and then led to expansion of the prehistorical prosperity to the modern steppe areas (Fig. 4C).

Our reliable PANN reconstructions also provide important climate insights when assessing human activities across the modern agro-pastoral ecotone. Recent excavations at Shimao site (4.3–3.8 cal ka BP) in Region 2 demonstrates this importance. Shimao is a late Neolithic city-

type and stone-walled central settlement on the Loess Plateau and Mu Us Sandy Land transitional zone and also the largest (ca. 4.25 km²) discovered prehistoric site in China to date (Sun et al., 2014). Rawson (2017) deemed that agricultural shortages caused by a drier climate played a significant role in the spread of Bronze Age technology from the Ordos steppe to Shimao, and then to the Central Plains. Our PANN curves indeed show a drier trend before the construction of Shimao and a severer drought after 3.8 cal ka BP, which coincides with the abandonment of Shimao (Fig. 4). Major archaeological sites in Region 2 also demonstrates a southward distribution after Yangshao era.

Environment deterioration after 4.0 cal ka BP led to diverse subsistence strategies along the Great Wall. After a widespread agriculture-based Qijia Culture (4.2–3.6 cal ka BP) in west Loess Plateau and Upper Yellow River Valley (Region 1), succeeded cultures had more stock-breeding features and diffused westward (An et al., 2005). For instance, agriculture development for Xindian Culture (3.6–2.6 cal ka BP) was lagged behind the contemporaneous cultures in Middle Yellow River Valley but stock-raising was greatly developed, while Siba Culture (3.9–3.4 cal ka BP) spread west into Hexi Corridor and Kayue Culture (3.6–2.5 cal ka BP) expanded west to the eastern margin of Qaidam Basin (Institute of Archaeology CASS, 2003, 2004). In West Liao River Basin (region 3), people subsisted on millet retreated southward, while people who chose animal husbandry and hunting migrated westward (Jia et al., 2016).

6. Conclusions

In this paper, we conduct quantitative Holocene climate reconstructions for six fossil pollen records from continental East Asia using modern analogue technique (MAT). Vegetation sensitivity index (VSI) introduced in this study alerts us that mosaic vegetation sensitivities to climate variables are highly heterogeneous at local and regional scales. VSI based regional climate coefficient patterns are consistent with pollen–climate relationships in calibration sets revealed by cross-validation and ordination, which both indicate that moisture regime is relatively more important for vegetation (pollen) distributions in monsoonal area, in particular, for the northern part. However, vegetation sensitivities to climate variables at local and regional scales are not always consistent. If vegetation mosaics are more sensitive to one variable (type) at both local and regional scales, the variable as a limited factor can be reliably reconstructed; if more than one or the importance is not consistent, the reconstructions are less plausible. Backward chaining a climate variable quantitatively from pollen data is not always reliable. We suggest that the procedure that we called local–regional–fossil comparison can be used to select appropriate climate variables.

In our cases, Holocene moisture reconstructions using fossil data from forest-steppe ecotone in North China can be trusted as their consistent importance in the comparisons. Holocene annual precipitation variations along the Great Wall demonstrate that the East Asian summer monsoon intensively influenced this transitional zone since 8.6 cal ka BP and retreated southward after 4.0 cal ka BP. The moisture condition change may have promoted the millet agriculture developments in North China around 8 cal ka BP and caused diverse subsistence strategy selections for past human society at the monsoon margin after 3.6 cal ka BP.

Acknowledgements

Special thanks to Z. Zheng (Sun Yat-sen University) and all other palynologists who have contributed to the East Asian Pollen Database. Fossil pollen data of Zoige Peatland are from the China West Pollen Database (<http://www.cpdw.net>) coordinated by Y. Zhao. This study was supported by the key program of National Natural Science Foundation of China (No. 41630753). The doctoral research of W. Ding at Freie Universität Berlin was funded by the China Scholarship Council

(No. 2011813072).

Appendix A. Supplementary data

Supplementary data related to this article can be found at <http://dx.doi.org/10.1016/j.quaint.2018.07.002>.

References

- Ackerly, D.D., Cornwell, W.K., Weiss, S.B., Flint, L.E., Flint, A.L., 2015. A geographic mosaic of climate change impacts on terrestrial vegetation: which areas are most at risk? *PLoS One* 10, e0130629. <https://doi.org/10.1371/journal.pone.0130629>.
- An, C.B., Tang, L., Barton, L., Chen, F., 2005. Climate change and cultural response around 4000 cal yr B.P. in the western part of Chinese Loess Plateau. *Quat. Res.* 63, 347–352. <https://doi.org/10.1016/j.yqres.2005.02.004>.
- Bennett, K.D., Willis, K.J., 2001. Pollen. In: Smol, J.P., Birks, H.J., Last, W.M. (Eds.), *Tracking Environmental Change Using Lake Sediments: Terrestrial, Algal, and Siliceous Indicators*. Kluwer Academic Publishers, Dordrecht.
- Birks, H.J.B., Birks, H.H., 1980. *Quaternary Palaeoecology*. Hodder Arnold, London.
- Birks, H.J.B., Heiri, O., Seppä, H., Bjune, A.E., 2010. Strengths and weaknesses of quantitative climate reconstructions based on Late-Quaternary biological proxies. *Open Ecol. J.* 3, 68–110. <https://doi.org/10.2174/1874213001003020068>.
- Cao, X., Tian, F., Telford, R.J., Ni, J., Xu, Q., Chen, F., Liu, X., Stebich, M., Zhao, Y., Hershuh, U., 2017. Impacts of the spatial extent of pollen-climate calibration-set on the absolute values, range and trends of reconstructed Holocene precipitation. *Quat. Sci. Rev.* 178, 37–53. <https://doi.org/10.1016/j.quascirev.2017.10.030>.
- Chen, F., Xu, Q., Chen, J., Birks, H.J., Liu, J., Zhang, S., Jin, L., An, C., Telford, R.J., Cao, X., Wang, Z., Zhang, X., Selvaraj, K., Lu, H., Li, Y., Zheng, Z., Wang, H., Zhou, A., Dong, G., Zhang, J., Huang, X., Bloemendal, J., Rao, Z., 2015. East Asian summer monsoon precipitation variability since the last deglaciation. *Sci. Rep.* 5 (11186). <https://doi.org/10.1038/srep11186>.
- Davis, B.A.S., Brewer, S., Stevenson, A.C., Guiot, J., 2003. The temperature of Europe during the Holocene reconstructed from pollen data. *Quat. Sci. Rev.* 22, 1701–1716. [https://doi.org/10.1016/s0277-3791\(03\)00173-2](https://doi.org/10.1016/s0277-3791(03)00173-2).
- deMenocal, P.B., 2001. Cultural responses to climate change during the late Holocene. *Science* 292, 667–673. <https://doi.org/10.1126/science.1059188>.
- Didan, K., 2015. MOD13C2: MODIS/Terra Vegetation Indices Monthly L3 Global 0.05 deg CMG V006. NASA EOSDIS Land Processes DAAC. <https://doi.org/10.5067/MODIS/MOD13C2.006>.
- Ding, W., Xu, Q., Tarasov, P.E., 2017. Examining bias in pollen-based quantitative climate reconstructions induced by human impact on vegetation in China. *Clim. Past* 13, 1285–1300. <https://doi.org/10.5194/cp-13-1285-2017>.
- Dong, G., Liu, F., Chen, F., 2017. Environmental and technological effects on ancient social evolution at different spatial scales. *Sci. China Earth Sci.* 60, 2067–2077. <https://doi.org/10.1007/s11430-017-9118-3>.
- Editorial Committee of Vegetation Map of China, C.A.S., 2007. *Vegetation Map of the People's Republic of China (1:1000000)*. Geological Publishing House, Beijing.
- Edwards, K.J., Fyfe, R.M., Jackson, S.T., 2017. The first 100 years of pollen analysis. *Native Plants* 3. <https://doi.org/10.1038/nplants.2017.1>.
- Fang, J., Ohsawa, M., Kira, T., 1996. Vertical vegetation zones along 30°N latitude in humid East Asia. *Vegetatio* 126, 135–149. <https://doi.org/10.1007/BF00045600>.
- Fick, S.E., Hijmans, R.J., 2017. WorldClim 2: new 1-km spatial resolution climate surfaces for global land areas. *Int. J. Climatol.* 37, 4302–4315. <https://doi.org/10.1002/joc.5086>.
- Forman, R.T.T., 1995. Some general principles of landscape and regional ecology. *Landscape Ecol.* 10, 133–142. <https://doi.org/10.1007/BF00133027>.
- Fu, C., Jiang, Z., Guan, Z., He, J., Xu, Z., 2008. *Regional Climate Studies of China*. Springer, Berlin.
- Gunin, P.D., Vostokova, E.A., Dorofeyuk, N.I., Tarasov, P.E., Black, C.C., 1999. Vegetation dynamics of Mongolia. In: Werger, M.J.A. (Ed.), *Geobotany*. Springer Netherlands, Dordrecht.
- Hershuh, U., Kürschner, H., Mischke, S., 2006. Temperature variability and vertical vegetation belt shifts during the last ~50,000 yr in the Qilian Mountains (NE margin of the Tibetan Plateau, China). *Quat. Res.* 66, 133–146. <https://doi.org/10.1016/j.yqres.2006.03.001>.
- Hill, M.O., Gauch, H.G., 1980. Detrended correspondence analysis: an improved ordination technique. *Vegetatio* 42, 47–58. <https://doi.org/10.1007/bf00048870>.
- Hong, D.-Y., Blackmore, S., 2015. *Plants of China: a Companion to the Flora of China*. Cambridge University Press, Cambridge.
- Hu, Y., Wang, S., Luan, F., Wang, C., Richards, M.P., 2008. Stable isotope analysis of humans from Xiaojingshan site: implications for understanding the origin of millet agriculture in China. *J. Archaeol. Sci.* 35, 2960–2965. <https://doi.org/10.1016/j.jas.2008.06.002>.
- Huete, A., Didan, K., Miura, T., Rodriguez, E.P., Gao, X., Ferreira, L.G., 2002. Overview of the radiometric and biophysical performance of the MODIS vegetation indices. *Remote Sens. Environ.* 83, 195–213. [https://doi.org/10.1016/s0034-4257\(02\)00096-2](https://doi.org/10.1016/s0034-4257(02)00096-2).
- Huntley, B., 2012. Reconstructing palaeoclimates from biological proxies: some often overlooked sources of uncertainty. *Quat. Sci. Rev.* 31, 1–16. <https://doi.org/10.1016/j.quascirev.2011.11.006>.
- Institute of Archaeology CASS, 2003. *Chinese Archaeology: Xia and Shang*, Archaeological Monograph Series Type A. China Social Sciences Press, Beijing.
- Institute of Archaeology CASS, 2004. *Chinese Archaeology: Western Zhou and Eastern Zhou*, Archaeological Monograph Series Type A. China Social Sciences Press, Beijing.
- Jackson, S.T., 2006. Vegetation, environment, and time: the origination and termination of ecosystems. *J. Veg. Sci.* 17, 549–557. <https://doi.org/10.1111/j.1654-1103.2006.tb02478.x>.
- Jackson, S.T., Blois, J.L., 2015. Community ecology in a changing environment: perspectives from the Quaternary. *Proc. Natl. Acad. Sci. Unit. States Am.* 112, 4915–4921. <https://doi.org/10.1073/pnas.1403664111>.
- Jia, X., Sun, Y., Wang, L., Sun, W., Zhao, Z., Lee, H.F., Huang, W., Wu, S., Lu, H., 2016. The transition of human subsistence strategies in relation to climate change during the Bronze Age in the West Liao River Basin, Northeast China. *Holocene* 26, 781–789. <https://doi.org/10.1177/0959683615618262>.
- Jiang, W., Guo, Z., Sun, X., Wu, H., Chu, G., Yuan, B., Hatté, C., Guiot, J., 2006. Reconstruction of climate and vegetation changes of Lake Bayanchagan (Inner Mongolia): Holocene variability of the East Asian monsoon. *Quat. Res.* 65, 411–420. <https://doi.org/10.1016/j.yqres.2005.10.007>.
- Juggins, S., 2013. Quantitative reconstructions in palaeolimnology: new paradigm or sick science? *Quat. Sci. Rev.* 64, 20–32. <https://doi.org/10.1016/j.quascirev.2012.12.014>.
- Juggins, S., 2015. *Rioja: Analysis of Quaternary Science Data*. 0.9–5 ed. <https://cran.r-project.org/package=r.ioja>.
- Leipe, C., Nakagawa, T., Gotanda, K., Müller, S., Tarasov, P.E., 2015. Late Quaternary vegetation and climate dynamics at the northern limit of the East Asian summer monsoon and its regional and global-scale controls. *Quat. Sci. Rev.* 116, 57–71. <https://doi.org/10.1016/j.quascirev.2015.03.012>.
- Li, J.Y., Xu, Q.H., Zheng, Z., Lu, H.Y., Luo, Y.L., Li, Y.C., Li, C.H., Seppä, H., 2015a. Assessing the importance of climate variables for the spatial distribution of modern pollen data in China. *Quat. Res.* 83, 287–297. <https://doi.org/10.1016/j.yqres.2014.12.002>.
- Li, M.Y., Xu, Q.H., Zhang, S.R., Li, Y.C., Ding, W., Li, J.Y., 2015b. Indicator pollen taxa of human-induced and natural vegetation in Northern China. *Holocene* 25, 686–701. <https://doi.org/10.1177/0959683614566219>.
- Li, Q., Lu, H., Zhu, L., Wu, N., Wang, J., Lu, X., 2011. Pollen-inferred climate changes and vertical shifts of alpine vegetation belts on the northern slope of the Nyainqentanglha Mountains (central Tibetan Plateau) since 8.4 kyr BP. *Holocene* 21, 939–950. <https://doi.org/10.1177/0959683611400218>.
- Li, Y.Y., Willis, K.J., Zhou, L.P., Cui, H.T., 2016. The impact of ancient civilization on the northeastern Chinese landscape: palaeoecological evidence from the Western Liaohe River Basin, Inner Mongolia. *Holocene* 16, 1109–1121. <https://doi.org/10.1177/0959683606069403>.
- Liu, H., Yin, Y., Wang, Q., He, S., Bruehlheide, H., 2015. Climatic effects on plant species distribution within the forest-steppe ecotone in northern China. *Appl. Veg. Sci.* 18, 43–49. <https://doi.org/10.1111/avsc.12139>.
- Liu, X., Jones, M.K., Zhao, Z., Liu, G., O'Connell, T.C., 2012. The earliest evidence of millet as a staple crop: new light on neolithic foodways in North China. *Am. J. Phys. Anthropol.* 149, 283–290. <https://doi.org/10.1002/ajpa.22127>.
- Lu, H., 2017. New methods and progress in research on the origins and evolution of prehistoric agriculture in China. *Sci. China Earth Sci.* 60, 2141–2159. <https://doi.org/10.1007/s11430-017-9145-2>.
- Lu, H.Y., Wu, N.Q., Liu, K.B., Zhu, L.P., Yang, X.D., Yao, T.D., Wang, L., Li, Q.A., Liu, X.Q., Shen, C.M., Li, X.Q., Tong, G.B., Jiang, H., 2011. Modern pollen distributions in Qinghai-Tibetan Plateau and the development of transfer functions for reconstructing Holocene environmental changes. *Quat. Sci. Rev.* 30, 947–966. <https://doi.org/10.1016/j.quascirev.2011.01.008>.
- Ma, Q.F., Zhu, L.P., Wang, J.B., Ju, J.T., Lu, X.M., Wang, Y., Guo, Y., Yang, R.M., Kasper, T., Habertzell, T., Tang, L.Y., 2017. *Artemisia/Chenopodiaceae* ratio from surface lake sediments on the central and western Tibetan Plateau and its application. *Palaeogeogr. Palaeoclimatol. Palaeoecol.* 479, 138–145. <https://doi.org/10.1016/j.palaeo.2017.05.002>.
- Mu, Q., Zhao, M., Running, S.W., 2011. Improvements to a MODIS global terrestrial evapotranspiration algorithm. *Remote Sens. Environ.* 115, 1781–1800. <https://doi.org/10.1016/j.rse.2011.02.019>.
- Nychka, D., Furrer, R., Paige, J., Sain, S., 2016. *fields: Tools for Spatial Data*. <https://doi.org/10.5065/D6W957CT>.
- Oksanen, J., Blanchet, F.G., Kindt, R., Legendre, P., Minchin, P.R., O'Hara, R.B., Simpson, G.L., Solymos, P., Stevens, M.H.H., Wagner, H., 2016. *Vegan: community ecology package*. <https://cran.r-project.org/package=vegan>.
- Olson, D.M., Dinerstein, E., Wikramanayake, E.D., Burgess, N.D., Powell, G.V.N., Underwood, E.C., D'Amico, J.A., Itoua, I., Strand, H.E., Morrison, J.C., Loucks, C.J., Allnutt, T.F., Ricketts, T.H., Kura, Y., Lamoreux, J.F., Wettengel, W.W., Hedau, P., Kassem, K.R., 2001. Terrestrial ecoregions of the world: a new map of life on Earth. *Bioscience* 51, 933–938. [0933:Teotwa]2.0.Co;2. [https://doi.org/10.1641/0006-3568\(2001\)051](https://doi.org/10.1641/0006-3568(2001)051).
- Overpeck, J.T., Webb, T., Prentice, I.C., 1985. Quantitative interpretation of fossil pollen spectra: dissimilarity coefficients and the method of modern analogs. *Quat. Res.* 23, 87–108. [https://doi.org/10.1016/0033-5894\(85\)90074-2](https://doi.org/10.1016/0033-5894(85)90074-2).
- Park, J., 2011. A modern pollen-temperature calibration data set from Korea and quantitative temperature reconstructions for the Holocene. *Holocene* 21, 1125–1135. <https://doi.org/10.1177/0959683611400462>.
- Prentice, I.C., Cramer, W., Harrison, S.P., Leemans, R., Monserud, R.A., Solomon, A.M., 1992. A global biome model based on plant physiology and dominance, soil properties and climate. *J. Biogeogr.* 19, 117–134. <https://doi.org/10.2307/2845499>.
- R Core Team, 2016. *R: A Language and Environment for Statistical Computing*. <https://www.r-project.org>.
- Rawson, J., 2017. Shimao and Erlitou: new perspectives on the origins of the bronze

- industry in central China. *Antiquity* 91, 1–5. <https://doi.org/10.15184/aqy.2016.234>.
- Salonen, J.S., Luoto, M., Alenius, T., Heikkilä, M., Seppä, H., Telford, R.J., Birks, H.J.B., 2014. Reconstructing palaeoclimatic variables from fossil pollen using boosted regression trees: comparison and synthesis with other quantitative reconstruction methods. *Quat. Sci. Rev.* 88, 69–81. <https://doi.org/10.1016/j.quascirev.2014.01.011>.
- Sang, G.-S., Li, F., Yang, X.-M., 2017. Significance of the Great wall of ming dynasty in Ordos plateau as geographical boundary (in Chinese). *Arid. Land Geogr.* 40, 485–493.
- Seddon, A.W., Macias-Fauria, M., Long, P.R., Benz, D., Willis, K.J., 2016. Sensitivity of global terrestrial ecosystems to climate variability. *Nature* 531, 229–232. <https://doi.org/10.1038/nature16986>.
- Shen, Z.-H., Fang, J.-Y., Chiu, C.-A., Chen, T.-Y., Liu, H.-Y., 2015. The geographical distribution and differentiation of Chinese beech forests and the association with *Quercus*. *Appl. Veg. Sci.* 18, 23–33. <https://dx.doi.org/10.1111/avsc.12108>.
- Song, Y.-C., Da, L.-J., 2016. Evergreen broad-leaved forest of East Asia. In: Box, E.O. (Ed.), *Vegetation Structure and Function at Multiple Spatial, Temporal and Conceptual Scales*. Springer, Cham.
- Stebich, M., Rehfeld, K., Schlütz, F., Tarasov, P.E., Liu, J., Mingram, J., 2015. Holocene vegetation and climate dynamics of NE China based on the pollen record from Sihailongwan Maar Lake. *Quat. Sci. Rev.* 124, 275–289. <https://doi.org/10.1016/j.quascirev.2015.07.021>.
- Sun, Z., Shao, J., Shao, A., Kang, N., Qu, F., Liu, X., 2014. The Shimao site in Shenmu county, Shaanxi. *Chin. Archaeol.* 14, 18–26. <https://doi.org/10.1515/char-2014-0003>.
- Tarasov, P.E., Guiot, J., Cheddadi, R., Andreev, A.A., Bezusko, L.G., Blyakharchuk, T.A., Dorofeyuk, N.I., Filimonova, L.V., Volkova, V.S., Zernitskaya, V.P., 1999. Climate in northern Eurasia 6000 years ago reconstructed from pollen data. *Earth Planet Sci. Lett.* 171, 635–645. [https://doi.org/10.1016/S0012-821X\(99\)00171-5](https://doi.org/10.1016/S0012-821X(99)00171-5).
- Telford, R.J., 2015. palaeoSig: Significance Tests of Quantitative Palaeoenvironmental Reconstructions. <https://cran.r-project.org/package=palaeoSig>.
- Telford, R.J., Birks, H.J.B., 2011. A novel method for assessing the statistical significance of quantitative reconstructions inferred from biotic assemblages. *Quat. Sci. Rev.* 30, 1272–1278. <https://doi.org/10.1016/j.quascirev.2011.03.002>.
- Tian, F., Cao, X., Dallmeyer, A., Ni, J., Zhao, Y., Wang, Y., Herzschuh, U., 2016. Quantitative woody cover reconstructions from eastern continental Asia of the last 22 kyr reveal strong regional peculiarities. *Quat. Sci. Rev.* 137, 33–44. <https://doi.org/10.1016/j.quascirev.2016.02.001>.
- Wagner, M., Tarasov, P., Hosner, D., Fleck, A., Ehrich, R., Chen, X., Leipe, C., 2013. Mapping of the spatial and temporal distribution of archaeological sites of northern China during the Neolithic and Bronze Age. *Quat. Int.* 290–291, 344–357. <https://doi.org/10.1016/j.quaint.2012.06.039>.
- Wang, H., Chen, J., Zhang, X., Chen, F., 2014. Palaeosol development in the Chinese Loess Plateau as an indicator of the strength of the East Asian summer monsoon: evidence for a mid-Holocene maximum. *Quat. Int.* 334–335, 155–164. <https://doi.org/10.1016/j.quaint.2014.03.013>.
- Wang, W., Feng, Z., 2013. Holocene moisture evolution across the Mongolian Plateau and its surrounding areas: a synthesis of climatic records. *Earth Sci. Rev.* 122, 38–57. <https://doi.org/10.1016/j.earscirev.2013.03.005>.
- Willis, K.J., Bailey, R.M., Bhagwat, S.A., Birks, H.J., 2010. Biodiversity baselines, thresholds and resilience: testing predictions and assumptions using palaeoecological data. *Trends Ecol. Evol.* 25, 583–591. <https://doi.org/10.1016/j.tree.2010.07.006>.
- Wu, W., Wang, X., Wu, X., Jin, G., Tarasov, P.E., 2014. The early Holocene archaeobotanical record from the Zhangmatun site situated at the northern edge of the Shandong Highlands, China. *Quat. Int.* 348, 183–193. <https://doi.org/10.1016/j.quaint.2014.02.008>.
- Xiao, J., Xu, Q., Nakamura, T., Yang, X., Liang, W., Inouchi, Y., 2004. Holocene vegetation variation in the Daihai Lake region of north-central China: a direct indication of the Asian monsoon climatic history. *Quat. Sci. Rev.* 23, 1669–1679. <https://doi.org/10.1016/j.quascirev.2004.01.005>.
- Xu, Q., Chen, F., Zhang, S., Cao, X., Li, J., Li, Y., Li, M., Chen, J., Liu, J., Wang, Z., 2017. Vegetation succession and east Asian summer monsoon changes since the last deglaciation inferred from high-resolution pollen record in Gonghai lake, Shanxi province, China. *Holocene* 27, 835–846. <https://doi.org/10.1177/0959683616675941>.
- Xu, Q.H., Cao, X.Y., Tian, F., Zhang, S.R., Li, Y.C., Li, M.Y., Li, J., Liu, Y.L., Liang, J., 2014. Relative pollen productivities of typical steppe species in northern China and their potential in past vegetation reconstruction. *Sci. China Earth Sci.* 57, 1254–1266. <https://doi.org/10.1007/s11430-013-4738-7>.
- Yi, M., Bettinger, R.L., Chen, F., Pei, S., Gao, X., 2014. The significance of Shuidonggou Locality 12 to studies of hunter-gatherer adaptive strategies in North China during the Late Pleistocene. *Quat. Int.* 347, 97–104. <https://doi.org/10.1016/j.quaint.2014.04.009>.
- Zhang, S., Xu, Q., Nielsen, A.B., Chen, H., Li, Y., Li, M., Hun, L., Li, J., 2012. Pollen assemblages and their environmental implications in the Qaidam Basin, NW China. *Boreas* 41, 602–613. <https://doi.org/10.1111/j.1502-3885.2012.00264.x>.
- Zhao, Y., Yu, Z., 2012. Vegetation response to Holocene climate change in East Asian monsoon-margin region. *Earth Sci. Rev.* 113, 1–10. <https://doi.org/10.1016/j.earscirev.2012.03.001>.
- Zhao, Y., Yu, Z., Zhao, W., 2011. Holocene vegetation and climate histories in the eastern Tibetan Plateau: controls by insolation-driven temperature or monsoon-derived precipitation changes? *Quat. Sci. Rev.* 30, 1173–1184. <https://doi.org/10.1016/j.quascirev.2011.02.006>.
- Zhao, Z., 2011. New archaeobotanical data for the study of the origins of agriculture in China. *Curr. Anthropol.* 52, S295–S306. <https://doi.org/10.1086/659308>.
- Zheng, Z., Wei, J., Huang, K., Xu, Q., Lu, H., Tarasov, P., Luo, C., Beaudouin, C., Deng, Y., Pan, A., Zheng, Y., Luo, Y., Nakagawa, T., Li, C., Yang, S., Peng, H., Cheddadi, R., Williams, J., 2014. East Asian pollen database: modern pollen distribution and its quantitative relationship with vegetation and climate. *J. Biogeogr.* 41, 1819–1832. <https://doi.org/10.1111/jbi.12361>.
- Zhu, C., Ma, C., Yu, S.-Y., Tang, L., Zhang, W., Lu, X., 2010. A detailed pollen record of vegetation and climate changes in Central China during the past 16000 years. *Boreas* 39, 69–76. <https://doi.org/10.1111/j.1502-3885.2009.00098.x>.